The Thermodynamic Evolution of the Hurricane Boundary Layer During Eyewall Replacement Cycles

Gabriel J. Williams, Jr.

Department of Physics and Astronomy, College of Charleston, Charleston, SC, USA

ABSTRACT

Eyewall replacement cycles (ERCs) are frequently observed during the lifecycle of mature tropical cyclones. Although the kinematic structure and intensity changes during an ERC have been well-documented, comparatively little research has been done to examine the evolution of the tropical cyclone boundary layer (TCBL) during an ERC. This study will examine how the inner core thermal structure of the TCBL is affected by the presence of multiple concentric eyewalls using a high-resolution moist, hydrostatic, multilayer diagnostic boundary layer model. Within the concentric eyewalls above the cloud base, latent heat release and vertical advection (due to the eyewall updrafts) dominate the heat and moisture budgets, whereas vertical advection (due to subsidence) and vertical diffusion dominate the heat and moisture budgets for the moat region. Furthermore, it is shown that the development of a moat region within the TCBL depends sensitively on the moat width in the overlying atmosphere and the relative strength of the gradient wind field in the overlying atmosphere. These results further indicate that the TCBL contributes to outer eyewall formation through a positive feedback process between the vorticity in the nascent outer eyewall, boundary layer convergence, and boundary layer moist convection.

INTRODUCTION

The kinematic structure and intensity changes during an ERC have been well-documented in numerical and observational studies. The kinematic structure of the TC inner core during an ERC consists of calm winds near the storm center that rapidly increases to a maximum at the inner eyewall. The outer eyewall, located at a distant radius from an existing primary inner eyewall, usually contains a secondary wind maximum with enhanced vorticity, and the region between the eyewall consists of a largely convection-free low-vorticity moat. There have been recent studies which examined the kinematic structure of the TCBL during an ERC and the role of the TCBL in initiating the formation of the outer wind maximum Recent work has also examined the thermodynamic changes of the hurricane inner core during an ERC.

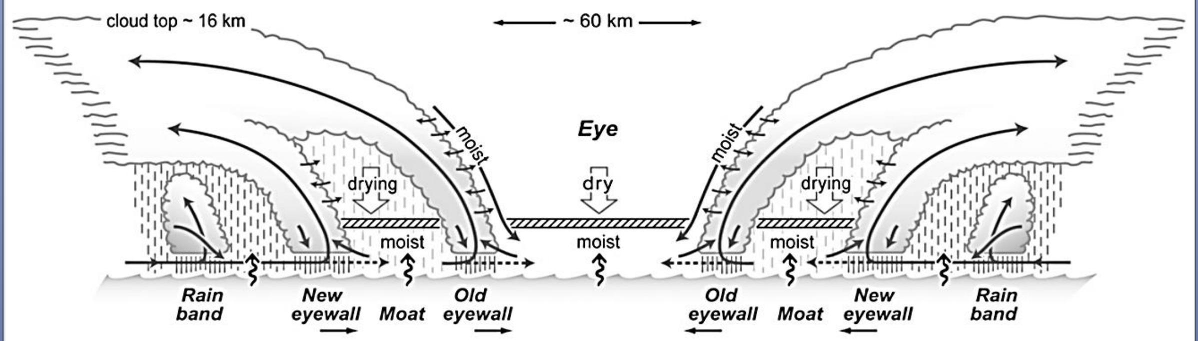

Conceptual Model of a TC undergoing an ERC. From Houze (2010)

Using flight-level data for 24 TCs, Sitkowski et al. (2012) examined the inner core thermodynamic changes during ERCs. Although much insight has been gained by the flight level (700-hPa) observational results of Sitkowski et al. (2012), boundary layer dynamics were not able to be investigated in this study. Furthermore, boundary layer dynamics were neglected in the balanced vortex frameworks used to interpret their results. Rather than focusing on the flight-level thermodynamic evolution and the radial flow aloft, this study will examine the boundary layer evolution during an ERC. In particular, this study will examine how the inner core thermal structure of the tropical cyclone boundary layer (TCBL) is affected by the presence of multiple concentric eyewalls using a high-resolution multilayer diagnostic boundary layer model.

NUMERICAL MODEL

The boundary layer model used here is an axisymmetric extension of the multilevel diagnostic boundary layer model used in Kepert and Wang (2001) and Williams (2015). Thus, the multilayer boundary model is based on the primitive equations for a moist, hydrostatic, Boussinesq atmosphere in cylindrical coordinates (r, z). Pertinent model details include

- Kessler warm rain microphysics scheme
- Louis PBL Scheme
- Standard bulk aerodynamic formulation for air-sea interaction
- Dissipative heating following Bryan and Rotunno (2009)
- Fairall et al. (1994) sea spray evaporation parameterization
- The wind field is initialized in gradient wind balance with the modified Rankine vortex model as in Sitkowski et al. (2011).
- The potential temperature field is initialized with a constant sea surface temperature of 302 K and a constant Brunt-Vaisala frequency of $10^{-2}\ s^{-1}$.
- The moisture field is initialized through a constant relative humidity of 85%.

For more information regarding numerical modeling details, see Williams (2016). Table 1 gives the parameters used for each model simulation.

Table 1 Parameters used in defining the vortices presented in this paper.

	r_1 (km)	v_1 (m s^{-1})	r_2 (km)	v_2 (m s^{-1})	r_M (km)
Vortex I	25	50	75	50	60
Vortex II	25	50	75	35	60
Vortex III	25	35	75	50	60
Vortex IV	40	50	75	50	60

The figure below gives the radial cross section from $r < 200\ km$ of the gradient wind profile for Vortex I (contour in blue), Vortex II (contour in green), Vortex III (contour in red), and Vortex IV (contour in black).

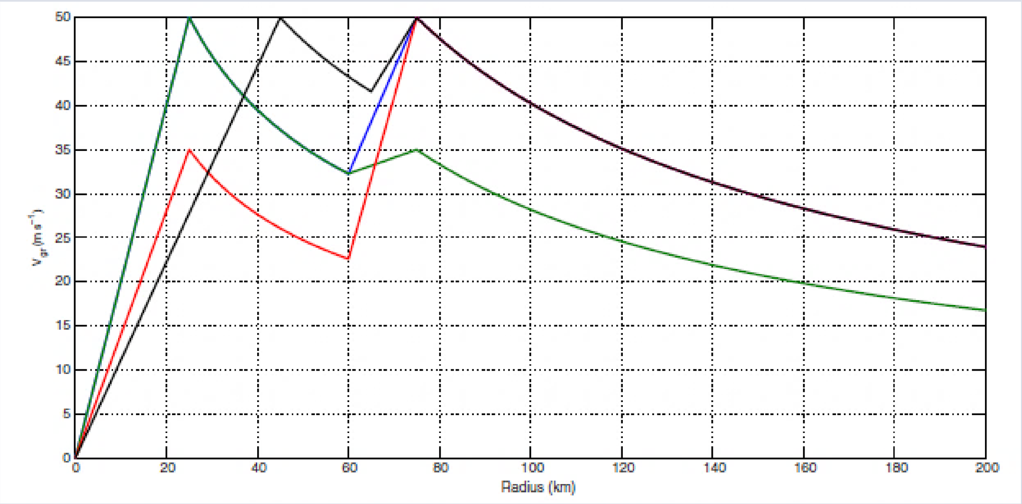

Vortex I is characteristic of a storm in which the concentric eyewalls are of similar strength. Vortex II is characteristic of a storm in which the outer eyewall strength is much weaker than the inner eyewall strength. Vortex III is characteristic of a storm in which the inner eyewall strength is much weaker than the outer eyewall strength. Vortex IV is similar to Vortex I, except the moat width has decreased.

RESULTS for VORTEX I and II

The figure below shows the steady-state thermal structure for Vortex I
.

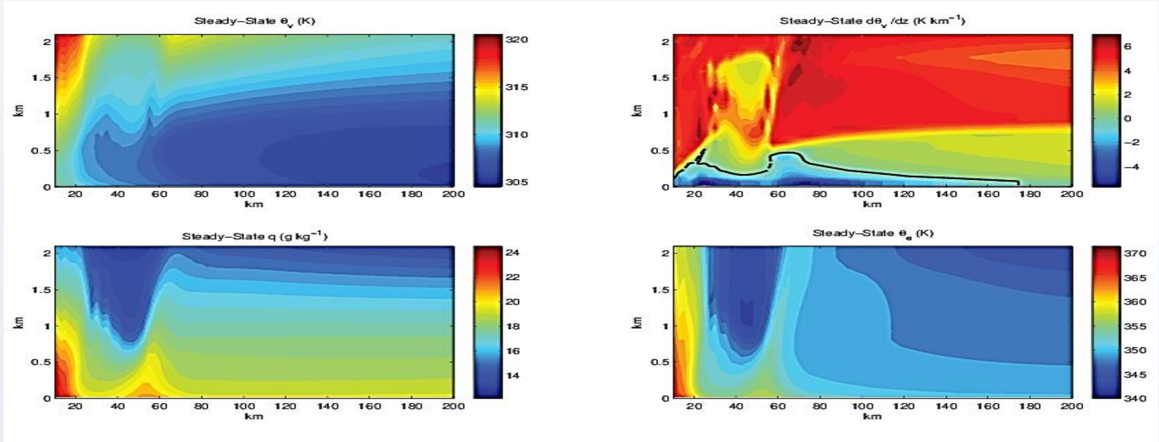

The thermodynamic budget analysis for the inner eyewall, the moat, the outer eyewall, and the skirt for Vortex I is given below.

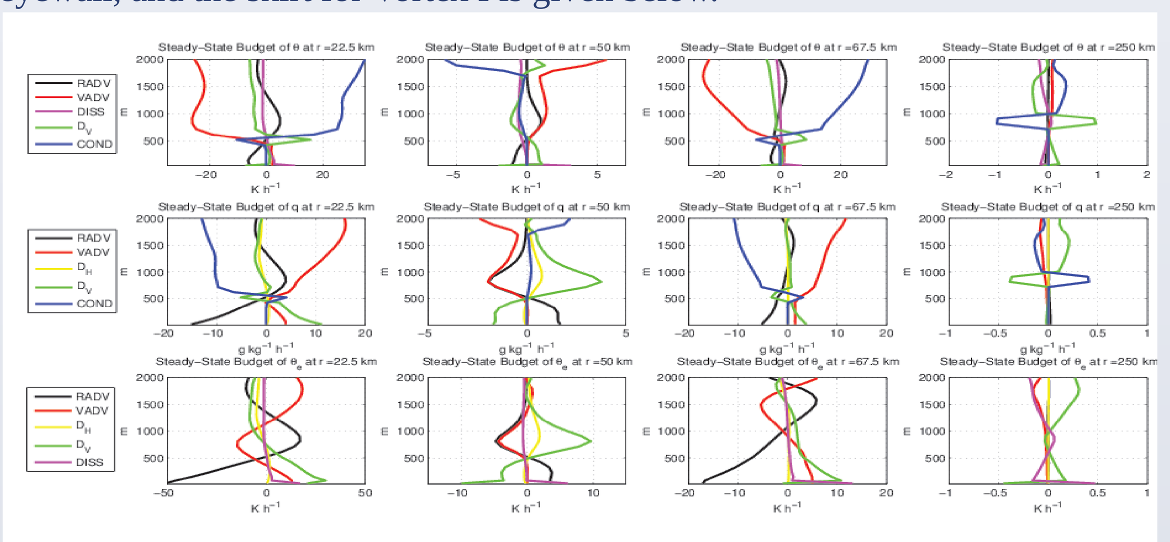

The figure below shows the steady-state thermal structure for Vortex II.

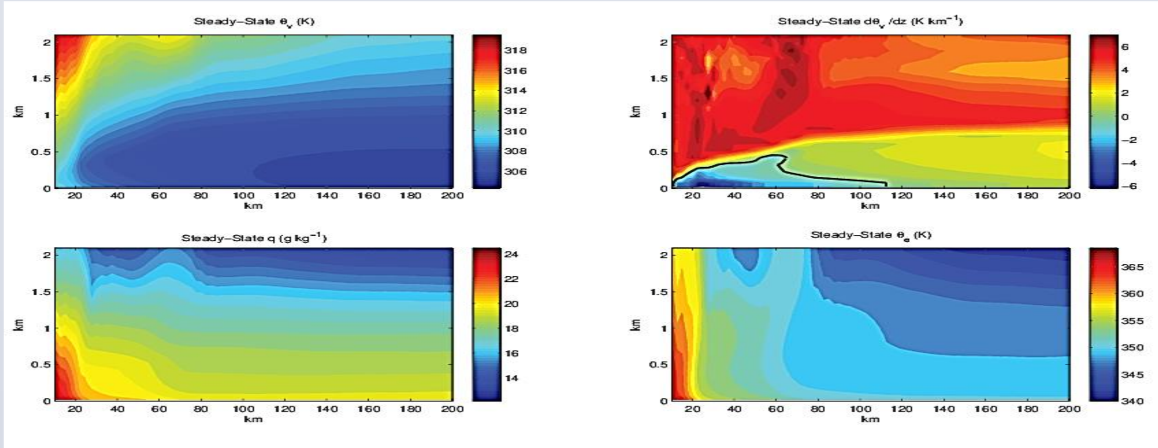

The thermodynamic budget analysis for the inner eyewall, the moat, the outer eyewall, and the skirt for Vortex II is given below.

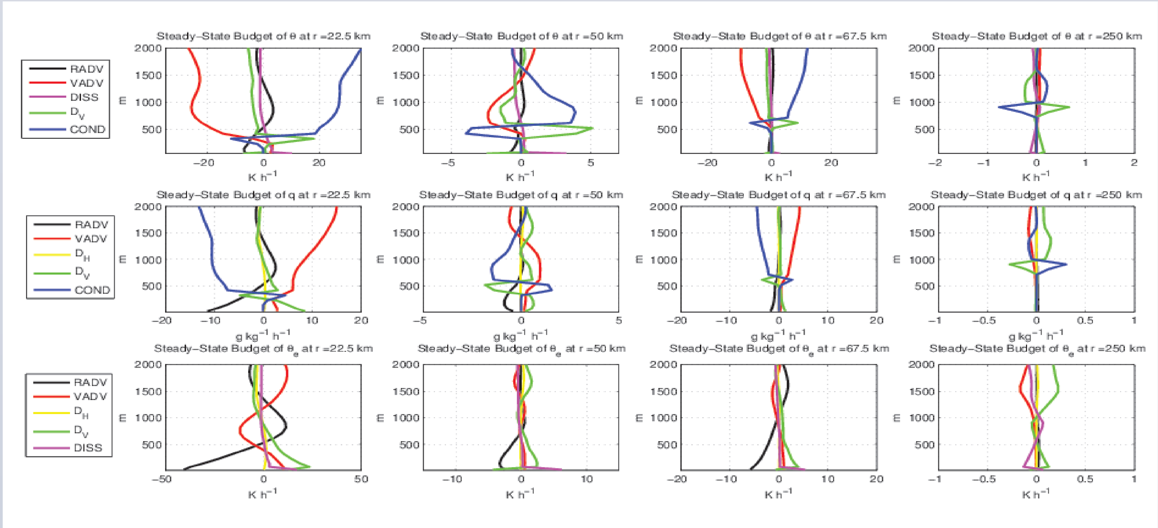

RESULTS for VORTEX III and IV

The figure below shows the steady-state thermal structure for Vortex III.

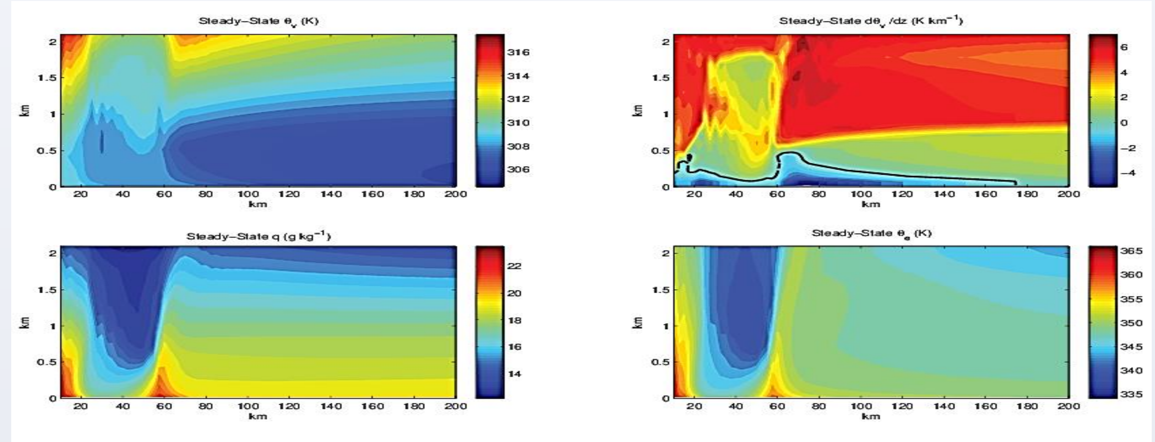

The thermodynamic budget analysis for the inner eyewall, the moat, the outer eyewall, and the skirt for Vortex III is given below.

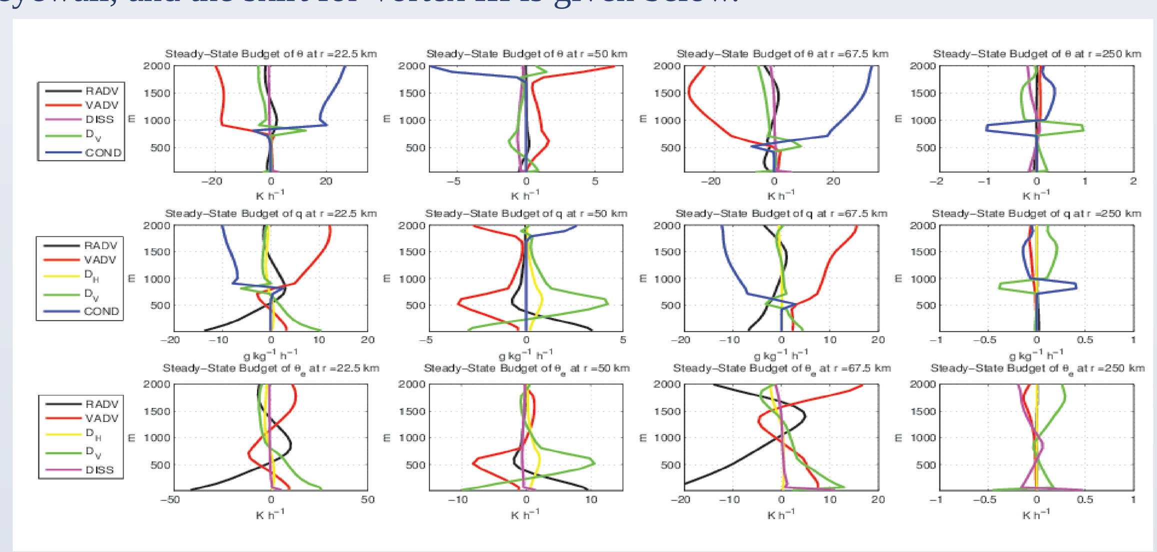

The figure below shows the steady-state thermal structure for Vortex IV – a storm in which moat width has decreased from 50 km to 35 km.

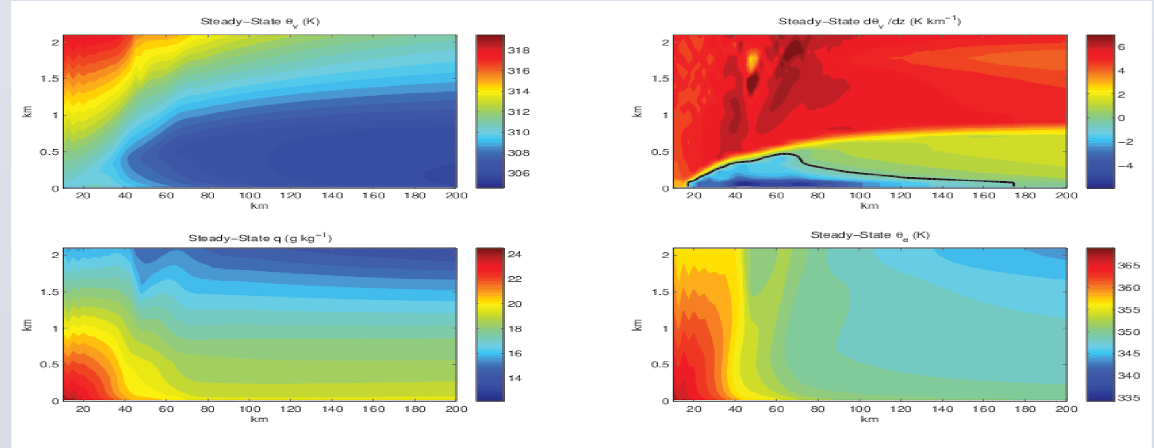

The thermodynamic budget analysis for the inner eyewall, the moat, the outer eyewall, and the skirt for Vortex IV is given below.

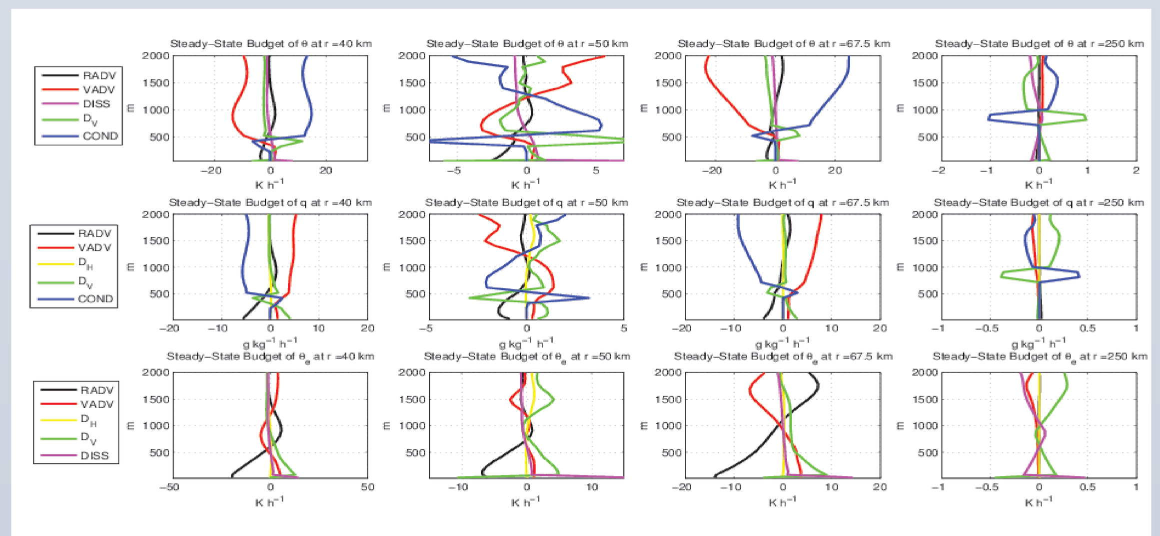

CONCLUSIONS

The main conclusions obtained from our simulations and diagnoses are as follows:

First, the import of dry air by warm subsidence tends to weaken the static stability within the moat region. Moreover, the vertical thermodynamic profiles within the moat region are more similar to the eye of the vortex with a deep layer of dry subsidence, a sharp vertical gradient in specific humidity, and small (yet positive) gradient in θ_v throughout the TCBL. Within the moat region above the inflow layer, both vertical and radial advection produces positive θ_v tendencies and negative q tendencies, which illustrates that the moat region is dominated by warm, dry subsidence.

Second, within both eyewalls, heat energy is dominated by latent heat release within the eyewall and upward surface sensible (and latent) heat fluxes from the underlying warm ocean and latent heating is primarily balanced by the cooling effect of vertical advection. Within the inflow (outflow) layer of the inner eyewall, radial advection provides a cooling (warming) effect, owing to inward (outward) motion and a negative radial gradient of θ. This change in sign, along with the change in sign of latent heating near the cloud base, serves to stabilize the boundary layer.

Third, the depth through which subsidence impinges upon the inflow layer depends upon relative strength of the inner eyewall to the outer eyewall and the moat width. Since the outer wind maxima resides in a region of lower vorticity, an outer eyewall with a substantially weaker wind maximum can produce a frictionally forced updraft as strong as the inner eyewall. However, the presence of a vorticity minimum in the moat increases the inner eyewall's updraft. These two effects are competing processes and the relative strength of the two eyewalls determines the depth of the subsidence. Moreover, a narrower moat decreases the strength of the secondary circulation associated with the inner eyewall, which decreases the depth of the subsidence within the moat region. A budget analysis of θ_e demonstrated that a reduced moat width, coupled with the lack of deep subsidence into the moat, tends to reduce the inward flux of moist entropy into the inner eyewall. Conversely, wider moats lead to a stronger and deeper subsidence within the moat region, which tends to preserve the frictionally forced updrafts in the inner eyewall.

REFERENCES

Fairall CW, Kepert JD, Holland GJ (1994) The effect of sea spray on surface energy transports over the ocean. Global Atmos Ocean Syst 2:121–142

Houze RA (2010) Clouds in tropical cyclones. J Atmos Sci 138:293-344.

Kepert JD, Wang Y (2001) The dynamics of boundary layer jets within the tropical cyclone core. Part II: nonlinear enhancement. J Atmos Sci 58:2485–2501

Sitkowski M, Kossin JP, Rozoff CM (2011) Intensity and structure changes during hurricane eyewall replacement cycles. Mon Weather Rev 139:3829–3847

Sitkowski M, Kossin JP, Rozoff CM, Knaff JA (2012) Hurricane eyewall replacement cycle thermodynamics and the relict inner eyewall circulation. J Atmos Sci 140:4035–4045.

Williams GJ Jr (2015) The effects of vortex structure and vortex translation on the tropical cyclone boundary layer wind field. J Adv Model Earth Syst 7:188–214.

Williams GJ Jr (2016) The thermodynamic evolution of the hurricane boundary layer during eyewall replacement cycles. Meteorol Atmos Phys